

Design of a Schiff Base Complex of Copper Coated on Epoxy-Modified Core–Shell MNPs as an Environmentally Friendly and Novel Catalyst for the One-Pot Synthesis of Various Chromene-Annulated Heterocycles

Sobhan Rezayati, Ali Ramazani,* Sami Sajjadifar, Hamideh Aghahosseini, and Aram Rezaei



Cite This: *ACS Omega* 2021, 6, 25608–25622



Read Online

ACCESS |



Metrics & More

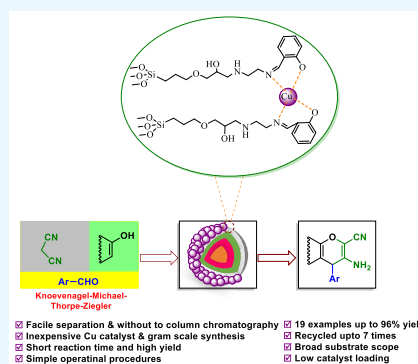


Article Recommendations



Supporting Information

ABSTRACT: An ecofriendly inorganic–organic hybrid and novel Schiff base complex of copper coated on epoxy-modified $\text{Fe}_3\text{O}_4@/\text{SiO}_2$ MNPs was successfully designed and prepared from readily available chemicals. In this method, a Schiff base complex as a linker is utilized to protect copper nanoparticles to the core–shell Fe_3O_4 exterior without agglomeration. The resulted Schiff base complex of copper coated on epoxy-modified $\text{Fe}_3\text{O}_4@/\text{SiO}_2$ MNPs was characterized and confirmed via different analyses such as FT-IR, TGA, XRD, VSM, FE-SEM, TEM, ICP, EDX, and BET. The novel catalyst was examined for the synthesis of various chromene-annulated heterocycles through the one-pot three component reaction of aromatic aldehydes, various phenols (2-hydroxynaphthalene-1,4-dione/resorcinol/ β -naphthol), and malononitrile in ethanol at reflux conditions. This method includes important aspects like no usage of column chromatography, very short reaction times, simplicity of product isolation using ethanol, excellent yields, simple procedures, and magnetic recoverability of the catalyst. All in all, our method makes a novel and significant advancement in the synthesis of various chromene-annulated heterocycles.



INTRODUCTION

Nowadays, the application of the fundamentals of green chemistry including application of green solvent, decreasing energy utilization and by-product, application of non-toxic substances, and usage of catalyst has attracted considerable attention. In the meantime, among the principles of green chemistry, the application of hybrid organic and inorganic materials as heterogeneous catalysts is most important.¹

In recent years, core–shell nanoparticles of Fe_3O_4 or $\gamma\text{-Fe}_2\text{O}_3$ are widely studied in various areas such as enzyme and protein separations,² environmental remediation,³ MRI contrast agent,⁴ magneto thermal therapy,^{5,6} drug delivery,^{7,8} bio separation,⁹ data storage,¹⁰ and biomolecular sensing.¹¹ Moreover, MNPs due to having a variety of notable advantages such as low cost, high surface area, superparamagnetism properties, high stability, convenient and cost-effective synthesis, separability, and reusability have become an increasing importance in organic synthesis.¹²

In the last decades, the synthesis and application of Schiff base complexes along with various ligand-coated core–shell magnetic nanoparticles in various sciences such as pharmaceutical and industrial fields have gained significant attention due to Schiff base complexes having a variety of advantages such as chemical inertness, high surface-to-volume ratios, environmentally friendly nature, proper thermal stability,

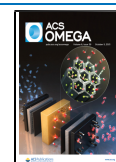
nontoxicity, effectuality, easy separability and reusability, and also merit to design for various uses.^{13–16}

4*H*-Chromene and their derivatives like 4*H*-pyran derivatives and 4*H*-pyran-annulated heterocyclic moieties are one of the primary classes of natural compounds, which include six-membered-ring heterocycles with oxygen. The synthesis of 4*H*-chromene and their derivatives have considerably drawn scientists' attention throughout the globe owing to their diverse biological and pharmaceutical activities like antifungal and antimicrobial,¹⁷ antitumor,¹⁸ anti-inflammatory,¹⁹ xanthine oxidase inhibiting,²⁰ anti-HIV,²¹ antiallergenic,^{22,23} antiproliferative and anticancer,^{22,24} and anti-rheumatic²⁵ (Scheme 1). Also, they have been used for the disease of Alzheimer, Huntington, and Parkinson.²⁶

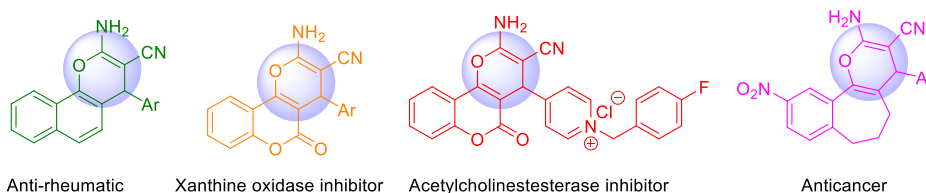
In addition, these compounds have attracted the attention of scientists especially medicinal and organic chemists to design, synthesize, and develop a lot of alkaloid compounds, for instance, huajiaosimuline and veprisine,^{27,28} (+)-calanolide

Received: July 13, 2021

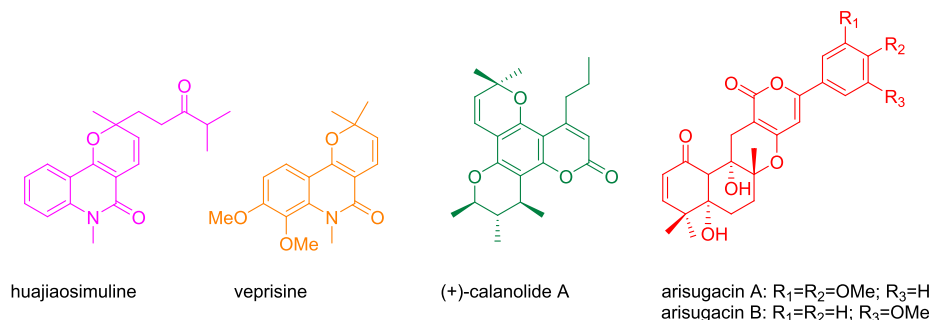
Published: September 14, 2021



Scheme 1. Examples of Chromene-Based Bioactive Compounds



Scheme 2. Selected Biologically Active Compounds Containing the Pyran-Annulated Motif



A,²⁹ and arisugacin,³⁰ which are examples of main pyran-annulated pharmacophoric scaffolds (Scheme 2).

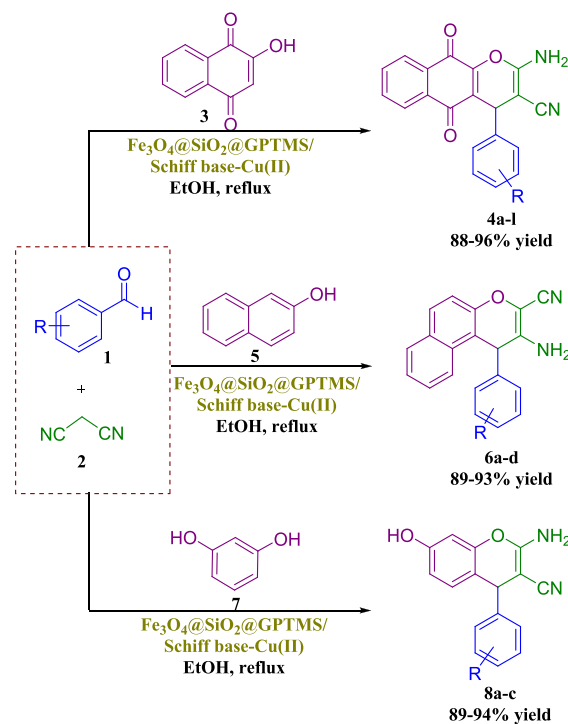
2-Amino-3-cyano-4*H*-chromene derivatives have been synthesized through a multicomponent reaction involving malononitrile,³¹ aldehyde, and enolizable C–H acids like dimedone, Kojic acid, barbituric acid, α - and β -naphthol, 2-hydroxy-1,4-naphthoquinone-4-hydroxy coumarin, and resorcinol in a one-pot reaction. It seems that the reaction was carried out to proceed through a Knoevenagel–Carba–Michael–Thorpe–Ziegler-type cascade method.³² Recently, various heterogeneous or homogeneous catalysts such as ionic liquids,³³ diammonium hydrogen phosphate (DAHP),³⁴ α -Fe₂O₃ nanoparticles,³⁵ H₆P₂W₁₈O₆₂·18H₂O,³⁶ cetrimonium bromide,³⁷ Mg–La mixed metal oxides,³⁸ silica-grafted ionic liquid,³⁹ TiCl₄,⁴⁰ InCl₃,⁴¹ triethylbenzylammonium chloride,⁴² Preyssler heteropoly acid,⁴³ and γ -alumina.⁴⁴ However, each of these approaches may have its own merits and some typical shortcomings like high cost, long reaction times, high temperature, usage of toxic solvent, low product yields, and difficulty of removal and recovery. Hence, the introduction of novel, eco-friendly, and simple heterogeneous catalysts is still valuable.

Therefore, based on the above-mentioned catalytic reaction conditions, herein, we now reported for the first time the synthesis, characterizations, and employment of novel Schiff base complexes of copper-coated core–shell MNPs (Fe₃O₄@SiO₂@GPTMS/Schiff base-Cu(II)) as a magnetically recoverable heterogeneous nanocatalyst for the preparation of 2-amino-4*H*-chromene derivatives through a one-pot three component reaction of aromatic aldehydes, various phenols (2-hydroxynaphthalene-1,4-dione/resorcinol/ β -naphthol), and malononitrile in ethanol at reflux conditions (Scheme 3).

RESULTS AND DISCUSSION

The Schiff base complex of copper coated on epoxy-modified Fe₃O₄@SiO₂ MNPs as a simple and environmentally friendly nanocatalyst was prepared by the immobilization of Schiff-base complex on core–shell magnetic nanoparticles followed by treatment with copper salt (Scheme 4). Then, the structure of the catalyst was characterized and confirmed using FT-IR,

Scheme 3. Synthesis of 2-Amino-4*H*-chromene Derivatives Catalyzed by the Schiff Base Complex of Copper Coated on Epoxy-Modified Fe₃O₄@SiO₂ MNPs



XRD, TGA, VSM, FE-SEM, TEM, ICP, EDX, and BET analysis.

As demonstrated in Figure 1, with a comparative style of each layer with the previous one, the FT-IR spectra of the Schiff base complex of copper coated on epoxy-modified Fe₃O₄@SiO₂ MNPs was investigated step by step. As can be seen in Figure 1a–f, a very strong peak at 610 cm⁻¹ is related to vibrations of Fe–O bonds of Fe₃O₄ and functionalized types of them. The FT-IR spectra of Fe₃O₄@SiO₂ show that the wide peak at 1106 cm⁻¹ confirms the existence of Si–O groups within the structure of the catalyst. After coating (3-

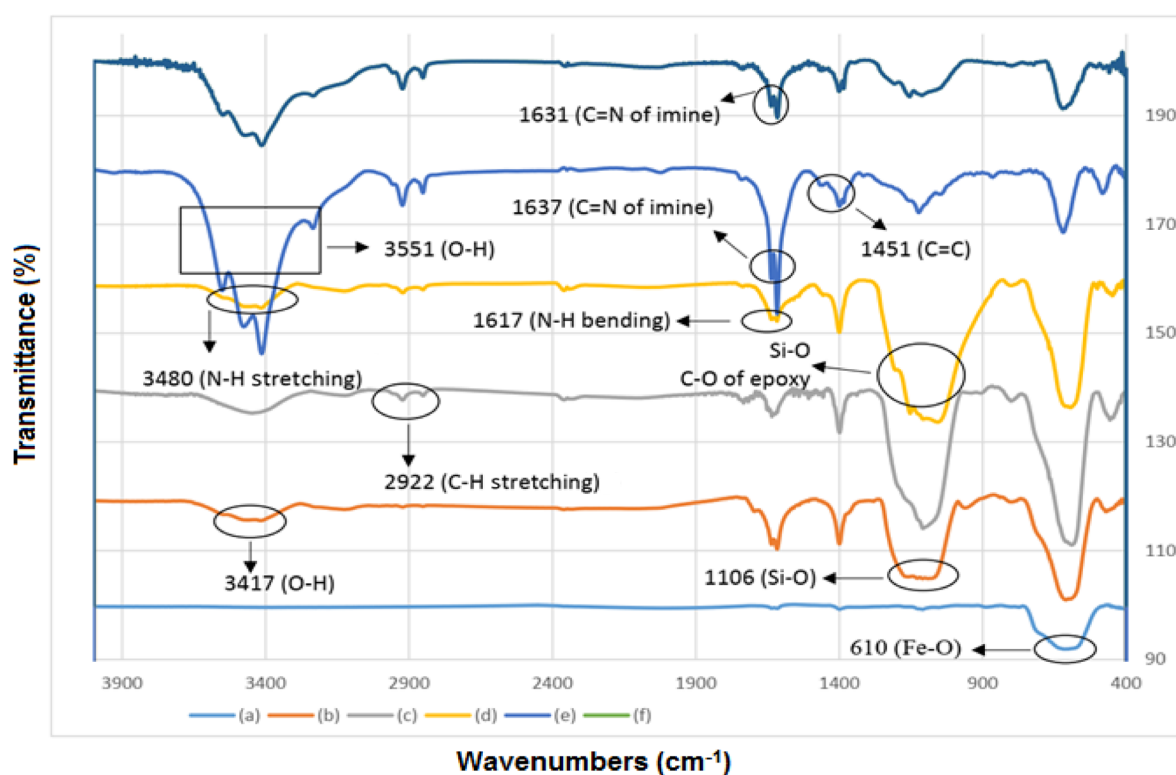
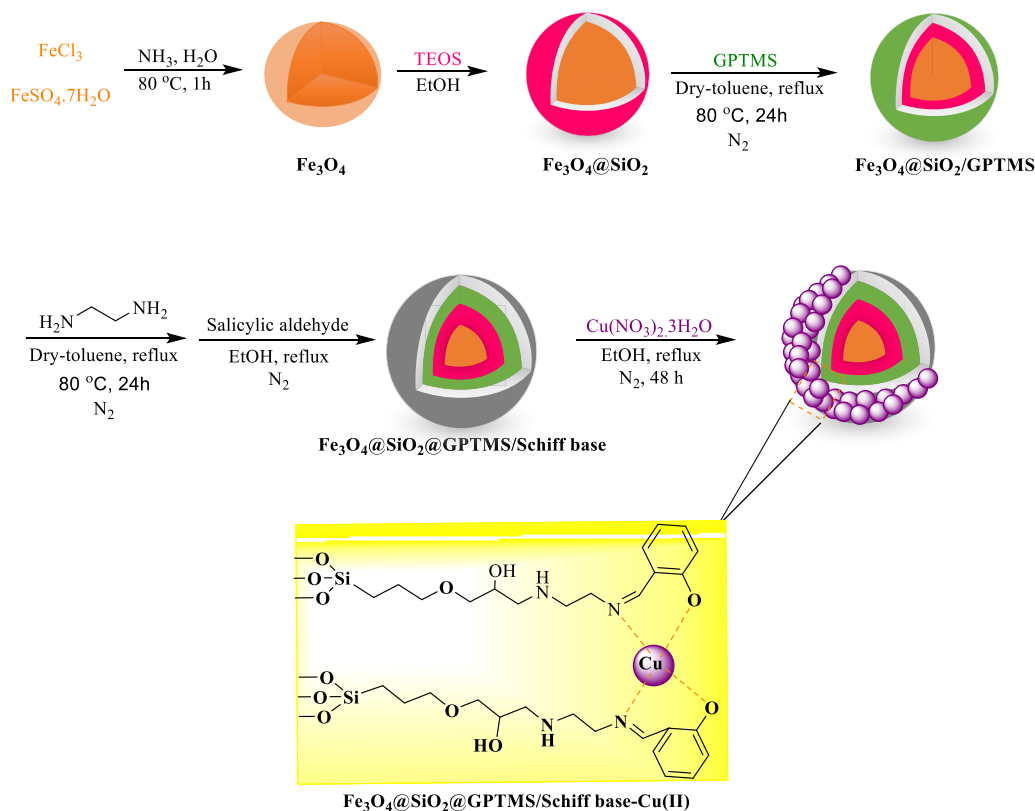
Scheme 4. Preparation of the Schiff Base Complex of Copper Coated on Epoxy-Modified Fe₃O₄@SiO₂ MNPs

Figure 1. FT-IR spectra of (a) Fe₃O₄, (b) Fe₃O₄@SiO₂, (c) Fe₃O₄@SiO₂-GPTMS, (d) Fe₃O₄@SiO₂-GPTMS@EDA, (e) Fe₃O₄@SiO₂-GPTMS/Schiff base, and (f) Fe₃O₄@SiO₂-GPTMS/Schiff base-Cu(II).

glycidylpropyl)trimethoxysilane (GPTMS) with Fe₃O₄@SiO₂ (Figure 1c), a new band appeared at 2922 cm⁻¹ that can be given to the alkyl CH₂ stretching vibration. Moreover,

characteristic absorption bands can be assigned to the epoxy group at 1108 cm⁻¹ that overlapped with the strong absorption of the bare silica.^{45,46} As expected, after the reaction between

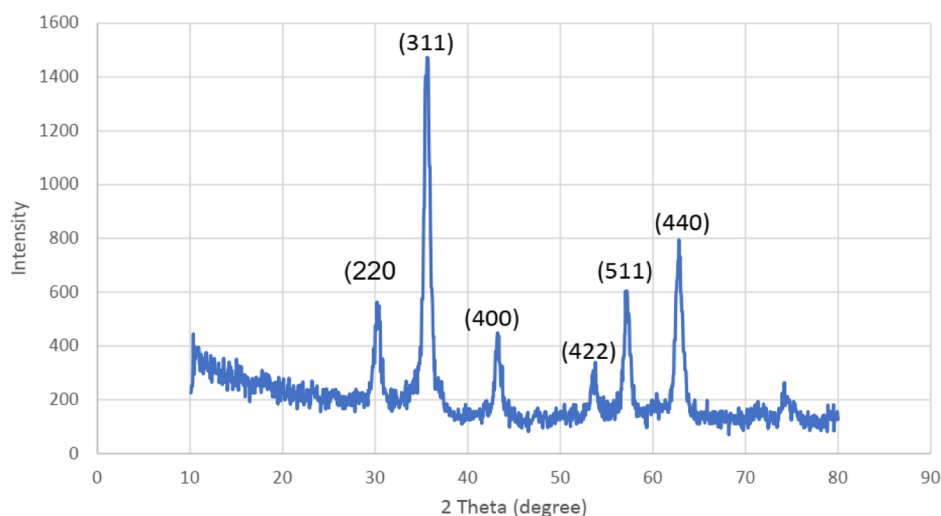


Figure 2. XRD patterns of the Schiff base complex of copper coated on epoxy-modified $\text{Fe}_3\text{O}_4@SiO_2$ MNPs.

$\text{Fe}_3\text{O}_4@SiO_2@GPTMS$ and diamine (Figure 1d), new absorption bands appear at 3480 and 1617 cm^{-1} , analogous to the nitrogen–hydrogen stretching frequency and bending vibration of nitrogen–hydrogen, respectively. The reaction of $\text{Fe}_3\text{O}_4@SiO_2@GPTMS/EDA$ with 2-hydroxybenzaldehyde produces $\text{Fe}_3\text{O}_4@SiO_2@GPTMS/Schiff$ base (Figure 1e). As can be seen in Figure 1e, new absorption bands appear at 3551 , 1637 , and 1451 cm^{-1} , analogous to the O–H stretching, stretching vibration of $C=N$, and stretching vibration of $C=C$, respectively. Moreover, after the reaction of $\text{Fe}_3\text{O}_4@SiO_2@GPTMS/Schiff$ base with $\text{Cu}(\text{NO}_3)_2 \cdot 3\text{H}_2\text{O}$, it produces a Schiff base complex of copper coated on epoxy-modified $\text{Fe}_3\text{O}_4@SiO_2$ MNPs (Figure 1f). It can be seen in Figure 2f that the wavenumber of $C=N$ in the Schiff base complex of copper coated on epoxy-modified $\text{Fe}_3\text{O}_4@SiO_2$ MNPs shifts to lower frequency (1631 cm^{-1}), which shows the coordination of metal–ligand bonds.^{47–49}

The crystalline structure of the Schiff base complex of copper coated on epoxy-modified $\text{Fe}_3\text{O}_4@SiO_2$ MNPs were measured with the XRD analysis at room temperature (Figure 2). As illustrated in Figure 2, the XRD pattern exhibited reflection peaks at $2\theta = 30.17$, 35.63 , 43.64 , 54.04 , 57.32 , and 63.08° , that are specified to the (220), (311), (400), (422), (511), and (440) crystallographic faces in well in line with the standard XRD pattern of cubic Fe_3O_4 (JCPDS 88-0866).⁵⁰ These results suggested the acceptable purity of the catalyst.

Figure 3a illustrates the magnetic properties of (a) Fe_3O_4 , (b) $\text{Fe}_3\text{O}_4@SiO_2$, (c) $\text{Fe}_3\text{O}_4@SiO_2@GPTMS$, (d) $\text{Fe}_3\text{O}_4@SiO_2@GPTMS/EDA$, (e) $\text{Fe}_3\text{O}_4@SiO_2@GPTMS/Schiff$ base, and (f) $\text{Fe}_3\text{O}_4@SiO_2@GPTMS/Schiff$ base-Cu(II) that were studied using a vibrating sample magnetometer (VSM) at room temperature. As a comparison, we decided to compare the saturation magnetization of Fe_3O_4 and the Schiff base complex of copper coated on epoxy-modified $\text{Fe}_3\text{O}_4@SiO_2$ MNPs with each other. The maximum saturation magnetization value of Fe_3O_4 was found to be about 58.5 emu/g , and the saturation magnetization value of the Schiff base complex of copper coated on epoxy-modified $\text{Fe}_3\text{O}_4@SiO_2$ MNPs was found to be about 27.7 emu/g ; this decrease is due to the successful coating of five layers on the surface of Fe_3O_4 MNP. As depicted in Figure 3a, all products had good magnetic properties, and this property is an important advantage of our catalyst for separation. Also, Figure 3b illustrates the separation

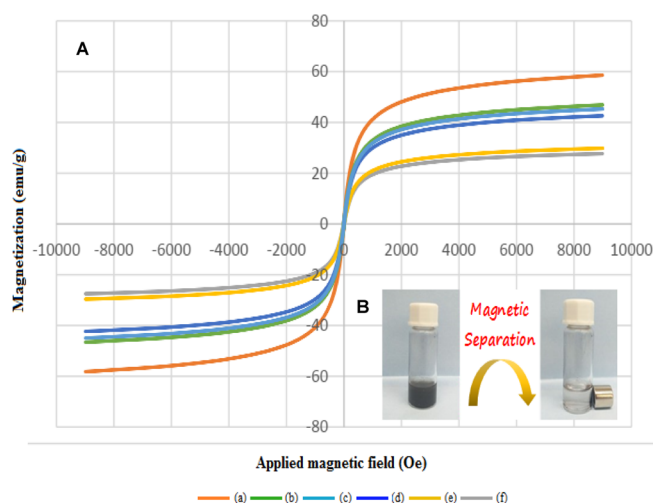


Figure 3. Magnetization curves for (a) Fe_3O_4 , (b) $\text{Fe}_3\text{O}_4@SiO_2$, (c) $\text{Fe}_3\text{O}_4@SiO_2@GPTMS$, (d) $\text{Fe}_3\text{O}_4@SiO_2@GPTMS/EDA$, (e) $\text{Fe}_3\text{O}_4@SiO_2@GPTMS/Schiff$ base, and (f) $\text{Fe}_3\text{O}_4@SiO_2@GPTMS/Schiff$ base-Cu(II).

of the Schiff base complex of copper coated on epoxy-modified $\text{Fe}_3\text{O}_4@SiO_2$ MNPs from the reaction mixture through an external magnet.

The thermo gravimetric analysis (TGA) of the Schiff base complex of copper coated on epoxy-modified $\text{Fe}_3\text{O}_4@SiO_2$ MNPs, $\text{Fe}_3\text{O}_4@SiO_2@GPTMS/Schiff$ base, $\text{Fe}_3\text{O}_4@SiO_2@GPTMS/EDA$, and $\text{Fe}_3\text{O}_4@SiO_2$ were investigated in the range of 25 – $800\text{ }^\circ\text{C}$ (Figure 4). The TGA curve of $\text{Fe}_3\text{O}_4@SiO_2@GPTMS/Schiff$ base-Cu(II) show that the first weight loss of 1% pertains to the removal of moisture contents at $110\text{ }^\circ\text{C}$. The second weight loss of 2% is related to the removal of the organic groups on the surface of Fe_3O_4 around $200\text{ }^\circ\text{C}$. Also, the third weight loss of 7% between 400 and $500\text{ }^\circ\text{C}$ is related to the removal of the organic compounds. It should be mentioned that the complete decomposition of the Schiff base complex of copper coated on epoxy-modified $\text{Fe}_3\text{O}_4@SiO_2$ MNPs appeared at $500\text{ }^\circ\text{C}$.

The energy dispersive X-ray (EDS) analysis of the Schiff base complex of copper coated on epoxy-modified $\text{Fe}_3\text{O}_4@SiO_2$ MNPs was investigated to show the adsorption of Cu on the surface of Fe_3O_4 and other organic contents in the

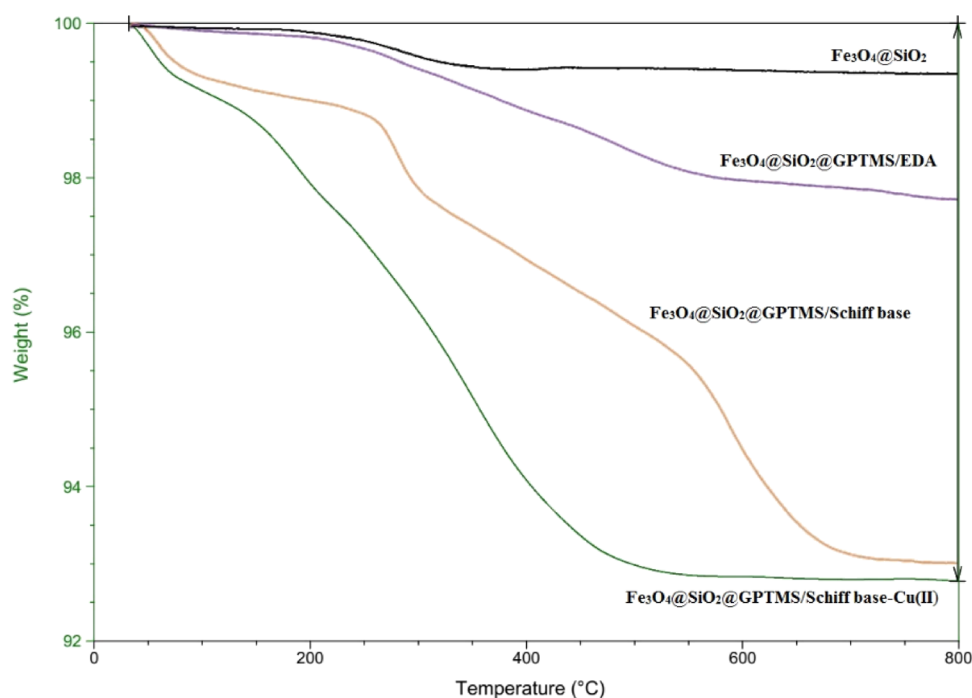


Figure 4. TGA diagram of the Schiff base complex of copper coated on epoxy-modified $\text{Fe}_3\text{O}_4@SiO_2$ MNPs, $\text{Fe}_3\text{O}_4@SiO_2@GPTMS/Schiff$ base, $\text{Fe}_3\text{O}_4@SiO_2@GPTMS/EDA$, and $\text{Fe}_3\text{O}_4@SiO_2$.

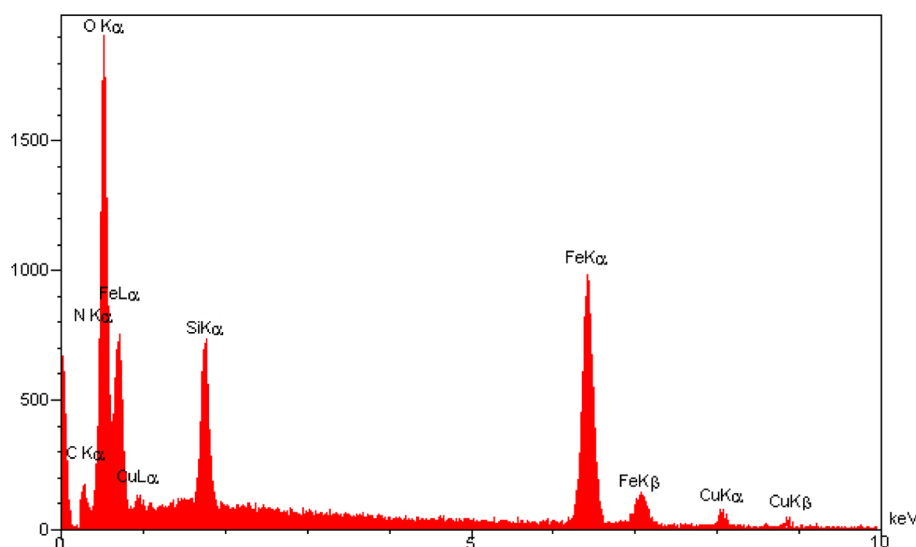


Figure 5. EDX image of the Schiff base complex of copper coated on epoxy-modified $\text{Fe}_3\text{O}_4@SiO_2$ MNPs.

structure of the nanocatalyst (Figure 5). The EDS image show that the peaks related to with iron, oxygen, nitrogen, carbon, silicium, and copper can be observed. In addition, it was found that the coating of copper on the surface of $\text{Fe}_3\text{O}_4@SiO_2@GPTMS/Schiff$ base was successful.

For the distribution of a variety of chemical elements in the nanocatalyst matrix, the wavelength-dispersive X-ray analysis (WDX) of the Schiff base complex of copper coated on the epoxy-modified $\text{Fe}_3\text{O}_4@SiO_2$ MNP catalyst is indicated in Figure 6. As shown in Figure 6, the WDX analysis shows that Cu is well distributed on the surface of the nanocatalyst.

To investigate the exact molar ratio of Cu in the Schiff base complex of copper coated on epoxy-modified $\text{Fe}_3\text{O}_4@SiO_2$ MNPs, ICP-OES analysis was applied and the exact amount of Cu in the catalyst has been calculated. According to the ICP

analysis, the exact amount of Cu in the Schiff base complex of copper coated on epoxy-modified $\text{Fe}_3\text{O}_4@SiO_2$ MNPs was 2.79 wt %.

To show the surface morphology, particle size, and particle shape of the synthesized Schiff base complex of copper coated on epoxy-modified $\text{Fe}_3\text{O}_4@SiO_2$ MNPs, the field-emission scanning electron microscopy image (FE-SEM) technique was conducted in various magnifications (Figure 7). As shown in the Figure 7, the prepared Schiff base complex of copper coated on epoxy-modified $\text{Fe}_3\text{O}_4@SiO_2$ MNPs was formed with a spherical morphology and an average size of 26–45 nm.

Figure 8 illustrate TEM images of the Schiff base complex of copper coated on epoxy-modified $\text{Fe}_3\text{O}_4@SiO_2$ MNPs. As illustrated in Figure 8, the TEM image confirmed that the amorphous silica (bright area) coated with successful on the

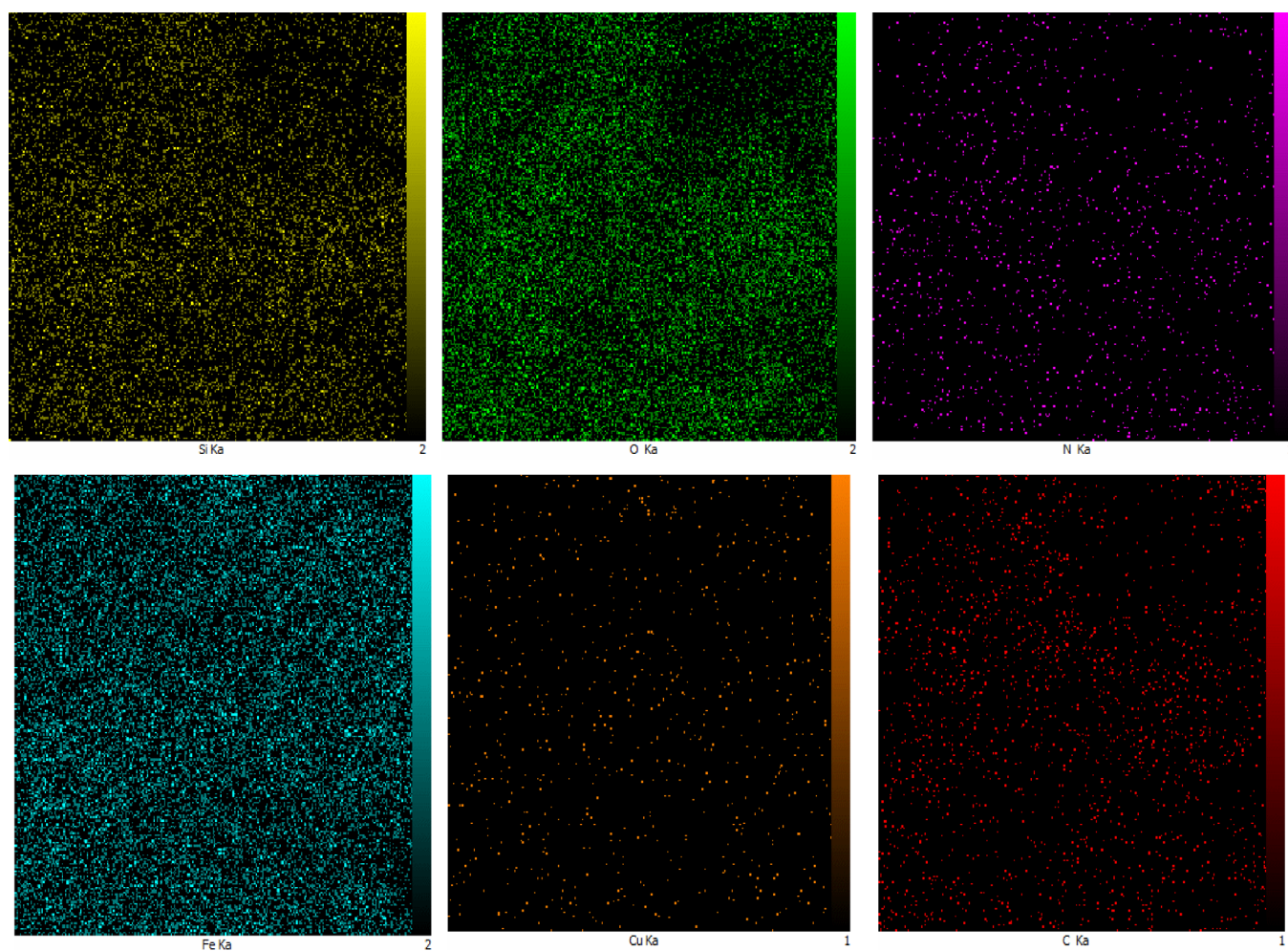


Figure 6. X-ray map analysis of the Schiff base complex of copper coated on epoxy-modified $\text{Fe}_3\text{O}_4@\text{SiO}_2$ MNPs.

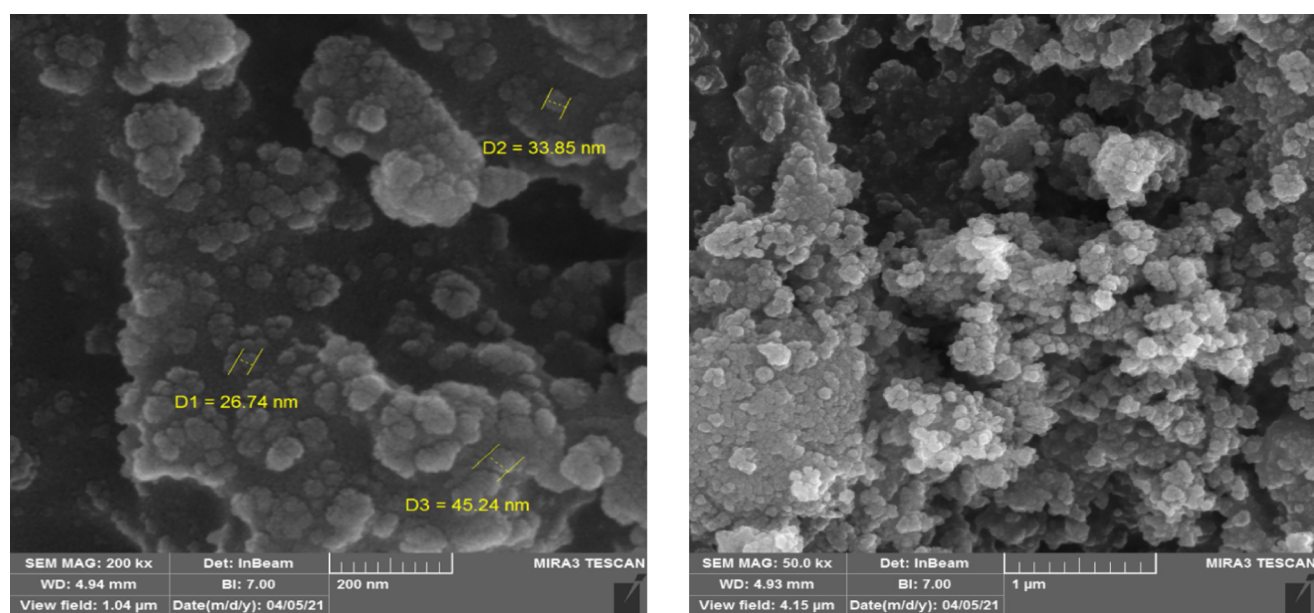


Figure 7. FE-SEM analysis of the Schiff base complex of copper coated on epoxy-modified $\text{Fe}_3\text{O}_4@\text{SiO}_2$ MNPs.

Fe_3O_4 magnetic nanoparticles (dark core). Furthermore, the average size of catalyst is approximately 26 to 45 nm, and the TEM revealed that nanoparticles with almost spherical.

Brunauer–Emmette–Teller (BET) analysis is an efficient technique to the measure of the surface area and pore volume of the adsorbent Schiff base complex of copper coated on

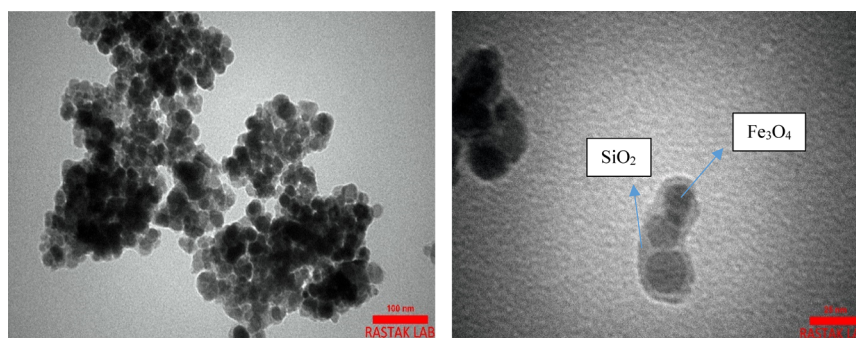


Figure 8. TEM analysis of the Schiff base complex of copper coated on epoxy-modified $\text{Fe}_3\text{O}_4@\text{SiO}_2$ MNPs.

epoxy-modified $\text{Fe}_3\text{O}_4@\text{SiO}_2$ MNPs. Figure 9a,b indicates its BET plot and nitrogen adsorption–desorption isotherms at a

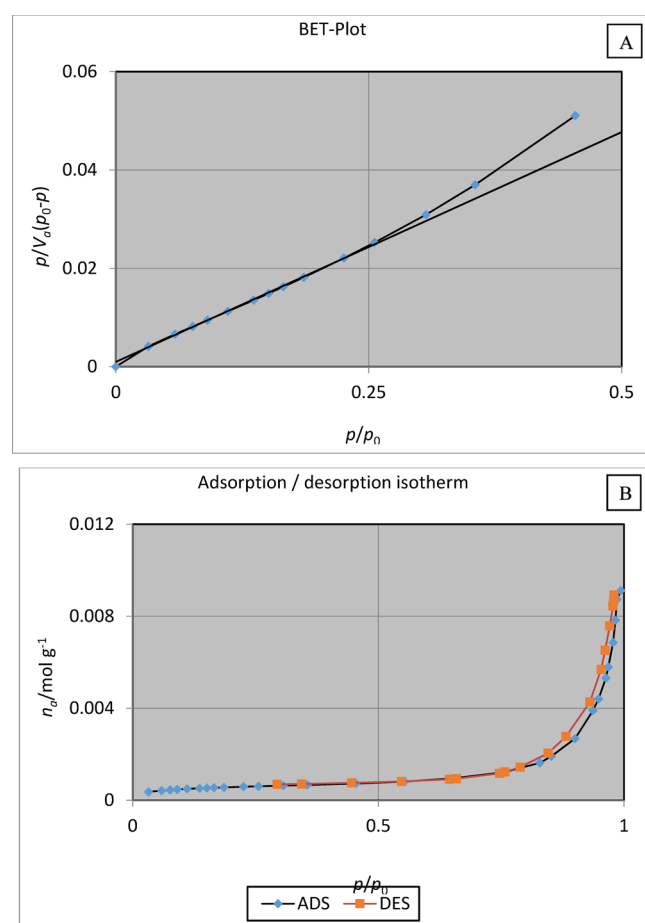


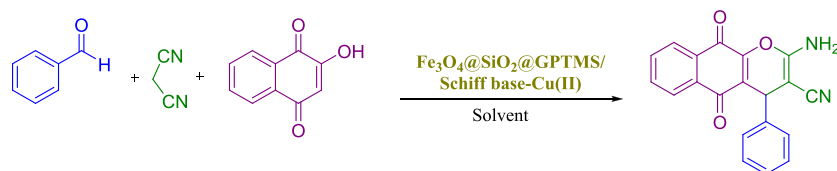
Figure 9. (a) BET plot of nitrogen adsorption. (b) BET plot of the nitrogen adsorption–desorption isotherms of the Schiff base complex of copper coated on epoxy-modified $\text{Fe}_3\text{O}_4@\text{SiO}_2$ MNPs.

temperature of 77 K. As illustrated Figure 9, the BET surface area, mean pore diameter, and total pore volume of the Schiff base complex of copper coated on epoxy-modified $\text{Fe}_3\text{O}_4@\text{SiO}_2$ MNPs were found to be $40.081 \text{ m}^2/\text{g}$, 26.94 nm , and $0.3104 \text{ cm}^3/\text{g}$, respectively. Also, according to IUPAC classification, our nanocatalyst is classified as a type IV isotherm, and the adsorbent is mesoporous.⁵¹

Catalytic Activity. Considering the Schiff base complex of copper coated on epoxy-modified $\text{Fe}_3\text{O}_4@\text{SiO}_2$ MNPs, as a magnetically recoverable and environmentally benign catalyst,

after its complete identification, we investigated its catalytic activity to synthesize a large number of 2-amino-4*H*-chromenes derivatives through the multicomponent reaction of benzaldehydes **1**, malononitrile **2**, and 2-hydroxynaphthalene-1,4-dione **3**, as a model reaction and then the impacts of different experimental parameters such as temperatures, solvents, and catalyst loading were investigated. For this study, the effect of the catalyst loading, temperature, and various solvents were investigated, and the summary of the discovered optimal conditions is presented in Table 1. The effect of various solvents such as EtOH, H_2O , $\text{H}_2\text{O}:\text{EtOH}$ (1:1), CH_3OH , CH_2Cl_2 , CH_3CN , toluene, and DMF, the catalyst amount (0.001 to 0.15 g), and temperature were investigated. It can be concluded that 0.05 g of $\text{Fe}_3\text{O}_4@\text{SiO}_2@\text{GPTMS}/\text{Schiff base-Cu(II)}$ is the needed amount of catalyst to create a 96% yield of **4a** in 10 min under reflux conditions (Table 1, entry 5). The reaction was done in the absence of $\text{Fe}_3\text{O}_4@\text{SiO}_2@\text{GPTMS}/\text{Schiff base-Cu(II)}$, and no conversion of product **4a** was found after 120 min at room temperature (Table 1, entry 1). In addition, the higher amount of the catalyst up to 0.1 and 0.15 g did not present their reaction time and better yields of **4a** (Table 1, entries 6–8). Both CH_3CN and toluene in the presence of 0.05 g of the Schiff base complex of copper coated on epoxy-modified $\text{Fe}_3\text{O}_4@\text{SiO}_2$ MNPs led to 40 and 45% of the **4a**, respectively (Table 1, entries 13 and 14). Moreover, the desired product **4a** was obtained in 10% and in trace amounts in the absence of $\text{Fe}_3\text{O}_4@\text{SiO}_2@\text{GPTMS}/\text{Schiff base-Cu(II)}$ in EtOH under reflux conditions and room temperature, respectively (Table 1, entries 16 and 17).

Subsequently, after getting the optimized conditions, derivatives of **4a–l** were synthesized through the reaction of electron-withdrawing or electron-donating substituents on the aromatic aldehydes, 2-hydroxynaphthalene-1,4-dione, and malononitrile in the presence of a magnetic nanocatalyst (0.05 g) in ethanol under reflux conditions (Table 2). Table 2 illustrates the corresponding products **4a–l** are obtained in 88–96% after 5–30 min. In another study, 0.05 g of the magnetic nanocatalyst successfully employed for the preparation of 3-amino-4-alkyl-1*H*-benzo[*f*]chromene-2-carbonitrile **6a–d**. Derivatives of **6a–d** were synthesized through the reaction of various aromatic aldehydes (benzaldehyde, 2,4-dichlorobenzaldehyde, 4-cyanobenzaldehyde, and 4-bromobenzaldehyde), β -naphthol, and malononitrile and are summarized in Table 2. Table 2 illustrates that the corresponding products **6a–d** are obtained in 89–93% after 20–25 min. Encouraged by these results, 0.05 g of the magnetic nanocatalyst successfully employed for the preparation of another major category of chromene-annulated heterocycles, namely, 2-amino-7-hydroxy-

Table 1. Optimization of the Catalyst Amount, Solvent, and Temperature for the Synthesis of 4a^a

entry	catalyst (g)	solvent	temperature (°C)	time (min)	yield (%) ^b	conv (%) ^c
1	no catalyst		r.t.	120	trace	0
2	0.005	EtOH	reflux	60	45	70
3	0.01	EtOH	reflux	30	65	81
4	0.03	EtOH	reflux	30	77	95
5	0.05	EtOH	reflux	10	96	100
6	0.07	EtOH	reflux	20	80	100
7	0.1	EtOH	reflux	20	75	100
8	0.15	EtOH	reflux	30	71	99
9	0.05	H ₂ O	reflux	30	55	100
10	0.05	H ₂ O:EtOH (1:1)	reflux	45	73	100
11	0.05	CH ₃ OH	reflux	60	70	97
12	0.05	CH ₂ Cl ₂	reflux	110	55	87
13	0.05	CH ₃ CN	reflux	110	40	85
14	0.05	toluene	reflux	120	45	66
15	0.05	DMF	reflux	100	53	75
16	no catalyst	EtOH	reflux	120	10	15
17	no catalyst	EtOH	r.t.	120	trace	0

^aReaction conditions: benzaldehyde (1 mmol), phenol (1 mmol), malononitrile (1 mmol), various solvents (2 mL). ^bIsolated yield. ^cConversions were calculated from the ¹H NMR spectrum of crude products.

4-alkyl-4H-chromene-3-carbonitrile **8a-c**. Derivatives of **8a-c** were synthesized through the reaction of various aromatic aldehydes (benzaldehyde, 3-nitrobenzaldehyde, and 4-nitrobenzaldehyde), resorcinol, and malononitrile and are summarized in Table 2. Table 2 illustrates that the corresponding products **8a-c** are obtained in 89–94% after 25–40 min.

Proposed Mechanism. A plausible mechanism to prepare 2-amino-4H-chromene derivatives via one-pot three-component condensation of aldehydes, malononitrile, and various phenols (2-hydroxynaphthalene-1,4-dione/resorcinol/ β -naphthol) in the presence of the Schiff base complex of copper coated on epoxy-modified Fe₃O₄@SiO₂ MNPs is shown in Scheme 5. The first step involved performing Knoevenagel product **C** through the Knoevenagel condensation reaction between various aldehydes **A** and malononitrile **B** in the presence of the Schiff base complex of copper coated on epoxy-modified Fe₃O₄@SiO₂ MNPs as a Lewis acid magnetic nanocatalyst. In the second step, the Michael addition of 2-hydroxynaphthalene-1,4-dione **D** with Knoevenagel product **C** gave intermediate **E**. In the last step, by enolization of intermediate **E**, intermediate **F** was produced, which under intramolecular nucleophilic cyclization gives the 2-amino-4H-chromene derivatives. Then, the Schiff base complex of copper coated on epoxy-modified Fe₃O₄@SiO₂ MNPs was removed by a magnetic field to the reaction cycle to reuse.

Reusability of the Schiff Base Complex of Copper Coated on Epoxy-Modified Fe₃O₄@SiO₂ MNPs. One of the important factors for the design of eco-friendly catalytic systems in both industrial and synthetic pathways is recyclability and reusability. In our method, the recyclability of the Schiff base complex of copper coated on epoxy-modified Fe₃O₄@SiO₂ MNPs was evaluated with the reaction of 4-nitrobenzaldehydes, 2-hydroxynaphthalene-1,4-dione, and malononitrile as the model reaction (Figure 10). After the reaction model was

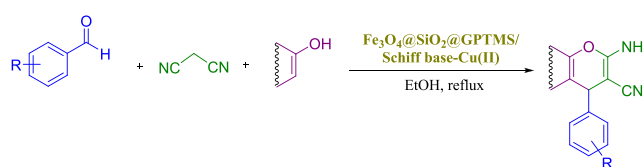
completed, the reaction mixture was cooled to room temperature and then the nanocatalyst can be isolated through an exterior magnet followed by washing with distilled water and EtOH, drying in air, and reusing directly for the subsequent reaction cycle.

Gram Scale Reaction. According to the excellent results obtained, the application of the current method has also been investigated in the gram scale (Scheme 6). For this purpose, the reaction of 4-nitrobenzaldehydes (10 mmol, 1.51 g), 2-hydroxynaphthalene-1,4-dione (10 mmol, 1.74 g), and malononitrile (10 mmol, 0.66 g) and also the reaction of 4-nitrobenzaldehydes (10 mmol, 1.51 g), resorcinol (10 mmol, 1.10 g), and malononitrile (10 mmol, 0.66 g) under optimized conditions have been investigated as model reactions. Scheme 6 illustrates that high yields of 86 and 85% were obtained for **4b** and **8c**, respectively.

Hot Filtration Test. A hot filtration experiment was conducted to study the heterogeneous nature and stability of the Schiff base complex of copper coated on epoxy-modified Fe₃O₄@SiO₂ MNPs. The hot filtration test aimed at the reaction of 4-nitrobenzaldehydes, 2-hydroxynaphthalene-1,4-dione, and malononitrile in the presence of a catalyst under optimized conditions. After half of the reaction time, 58% of the reaction was obtained. Subsequently, we repeated the above reaction under the same reaction and in half-time of the reaction, the Schiff base complex of copper coated on epoxy-modified Fe₃O₄@SiO₂ MNPs was separated from the reaction mixture and allowed to continue reaction without a nanocatalyst for a further time. It exhibits that only 58% of 2-amino-4-(4-nitrophenyl)-5,10-dioxo-5,10-dihydro-4H-benzo[*g*]-chromene-3-carbonitrile was obtained. These results clearly show that leaching of Cu has not occurred.

More importantly, the catalytic activity of this Schiff base complex of copper coated on epoxy-modified Fe₃O₄@SiO₂

Table 2. Preparation of 2-Amino-4*H*-chromene Derivatives Using the Schiff Base Complex of Copper Coated on Epoxy-Modified Fe₃O₄@SiO₂ MNPs^a



Entry	Product	Time (min)	Yield (%) ^b	Melting point (°C)		Entry	Product	Time (min)	Yield (%) ^b	Melting point (°C)	
				Found	reported					Found	reported
1		10	96	262-264	265 ⁵³	11 ^{New}		15	90	282-284	-
2		5	94	231-233	232 ⁵³	12		30	88	243-245	-
3		15	93	240-242	245 ⁵³	13		25	90	279-281	270 ⁵³
4		10	95	250-252	255 ⁵³	14		25	92	227-229	230 ⁵³
5		10	95	282-284	280-282 ⁵⁴	15		20	89	281-283	280-282 ⁵⁵
6		12	92	239-241	243 ⁵³	16		25	93	238-240	239-241 ⁵⁶
7		15	91	259-261	262 ⁵³	17		30	90	228-231	229-232 ⁵⁶
8		12	93	281-283	-	18		40	89	167-169	171-173 ⁵⁶
9		8	89	251-253	250 ⁵³	19		25	94	210-212	211-213 ⁵⁶
10 ^{New}		15	90	278-280	-						

^aReaction conditions: various aldehyde (1 mmol), phenol (1 mmol), malononitrile (1 mmol), phenol (1 mmol), catalyst (0.05 g), and EtOH (2 mL) reflux conditions. ^bIsolated yield.

MNPs was scrutinized in comparison with the catalytic activities of the Fe₃O₄@SiO₂@GPTMS/Schiff base, Fe₃O₄@

SiO₂@GPTMS, Fe₃O₄, Schiff base alone, and the Schiff base complex. Hence, the reaction of 4-nitrobenzaldehydes (1

Scheme 5. A Suggested Mechanism to Synthesize 2-Amino-4H-chromene Derivatives Catalyzed by the Schiff Base Complex of Copper Coated on Epoxy-Modified $\text{Fe}_3\text{O}_4/\text{SiO}_2$ MNPs

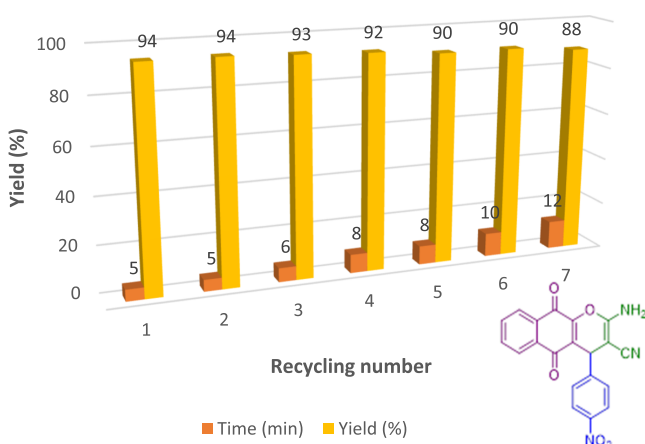
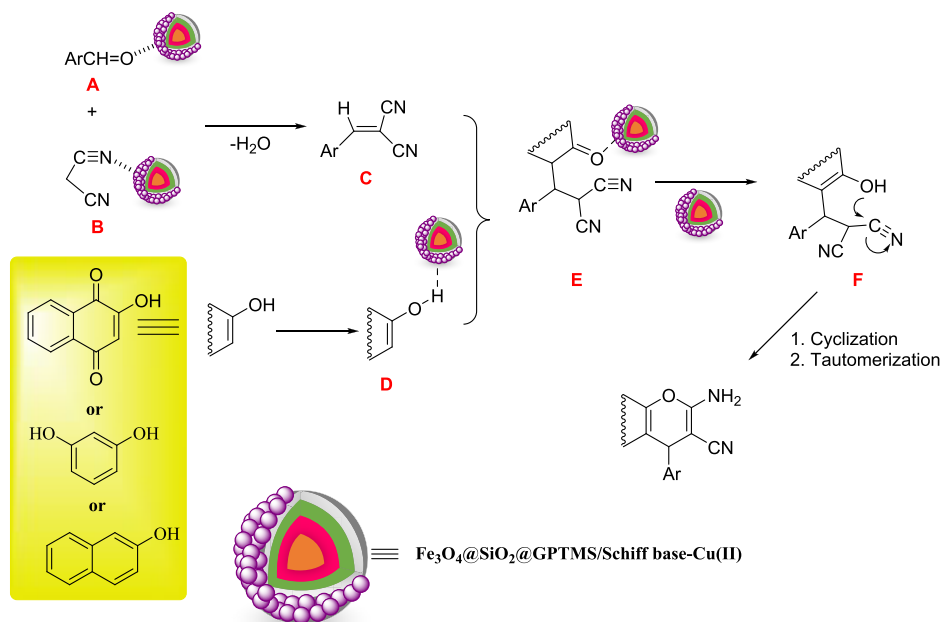
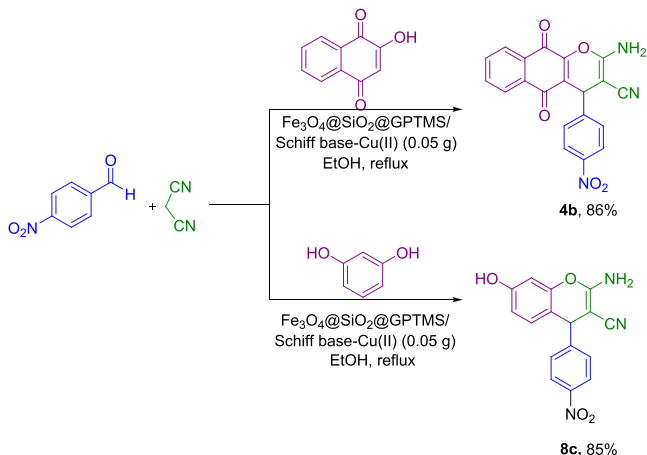


Figure 10. Recyclability of the catalyst.

Scheme 6. Comparison of Compounds 4b and 8c at Various Scales

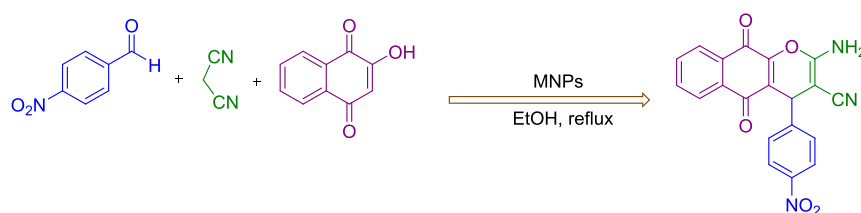


mmol), 2-hydroxynaphthalene-1,4-dione (1 mmol), and malononitrile in ethanol under reflux conditions has been investigated as the model reaction (Table 3). As shown in Table 3, the results clearly demonstrated that the $\text{Fe}_3\text{O}_4/\text{SiO}_2/\text{GPTMS}/\text{Schiff base-Cu(II)}$ MNPs in the model reaction gives strong results, and the corresponding product is formed in 96% yield after 10 min. On the other hand, the $\text{Fe}_3\text{O}_4/\text{SiO}_2/\text{GPTMS}/\text{Schiff base}$, $\text{Fe}_3\text{O}_4/\text{SiO}_2/\text{GPTMS}$, Fe_3O_4 , Schiff base, and Schiff base complex in the model reaction gives poor results, and the corresponding product is formed in low yields. These results clearly indicated that the enhanced activity is due to the presence of the Cu coated on $\text{Fe}_3\text{O}_4/\text{SiO}_2/\text{GPTMS}/\text{Schiff base}$. Also, the Schiff base alone was investigated for the model reaction. Three hours after the reaction, the desired product was not obtained at all (Table 3, entry 5). Moreover, when the Schiff base complex was replaced with Schiff base, the desired product was obtained in 53% yields after 90 min (Table 3, entry 6). Eventually, Fe_3O_4 (Table 3, entry 4) and $\text{Fe}_3\text{O}_4/\text{SiO}_2/\text{GPTMS}$ (Table 3, entry 3) gave the desired product 45 and 35%, respectively. It seems that the Fe_3O_4 can catalyze the reaction through the presence of OH-free groups on the surface. However, this effect is low in $\text{Fe}_3\text{O}_4/\text{SiO}_2/\text{GPTMS}$ than in Fe_3O_4 because the coating of various groups on the surface of the Fe_3O_4 led to the unavailability of the OH groups.

CONCLUSIONS

A novel Schiff base complex of copper coated on epoxy-modified $\text{Fe}_3\text{O}_4/\text{SiO}_2$ MNPs was successfully synthesized from readily-available chemicals. The magnetic nanoparticles exhibited high activity in the synthesis of various chromene-annulated heterocycles via a variety of aromatic aldehydes, various phenols (2-hydroxynaphthalene-1,4-dione/resorcinol/ β -naphthol), and malononitrile in EtOH at under reflux conditions. One of the factors of the high activity of this nanocatalyst may be the small size of the nanocatalyst between 26 and 45 nm, which leads to the dispersion and diffusion of the nanocatalyst in the reaction mixture. Simplicity of product

Table 3. Comparative Catalytic Activity of the Schiff Base Complex of Copper Coated on Epoxy-Modified Fe₃O₄@SiO₂ MNPs under Optimized Conditions



entry	catalyst	time (min)	yield (%) ^a
1	Fe ₃ O ₄ @SiO ₂ @GPTMS/Schiff base-Cu(II)	25	94
2	Fe ₃ O ₄ @SiO ₂ @GPTMS/Schiff base	360	33
3	Fe ₃ O ₄ @SiO ₂ @GPTMS	240	35
4	Fe ₃ O ₄	60	45
5	Schiff base alone	180	no reaction
6	Schiff base complex	90	53

^aIsolated yield.

isolation using ethanol, simple procedures, excellent yields, short reaction time, and no usage of column chromatography are notable advantages of these methods. More importantly, the nanocatalyst can be rapidly taken out from the reaction mixture with the help of an external magnet and after washing with ethanol, drying, and directly reusing in seven sequential runs without any loss in activity.

EXPERIMENTAL SECTION

Chemicals and Instrumentation. The materials used here including FeSO₄·7H₂O, FeCl₃, aqueous ammonia (25%), acetone, ethanol, tetraethyl orthosilicate, GPTMS, various aromatic aldehydes, toluene (anhydrous), various phenoles, ethylenediamine, malononitrile, salicylaldehyde, and Cu(NO₃)₂·3H₂O were prepared from the Merck or Fluka (Switzerland) Company. ¹H NMR (250 MHz) and ¹³C NMR (62.5 MHz) spectra using dimethyl sulfoxide (DMSO-*d*₆) were acquired on a Bruker DRX-250 AVANCE spectrometer. FT-IR analysis was fulfilled by a Perkin–Elmer 597 spectrophotometer. SEM analysis was recorded by a TESCAN, Brno Czech Republic. TEM analysis was recorded on a Zeiss EM10C operating at 80 kV TEM. The VSM analysis was utilized to specify the magnetic trait of the Schiff base complex of copper coated on epoxy-modified Fe₃O₄@SiO₂ MNPs (VSM, Taban, Tehran, Iran). Also, XRD analysis (X'Pert-PRO advanced diffractometer operated at 40 kV and 40 mA at r.t.) helped to investigate the crystalline structure of the catalyst. The EDAX spectrum was utilized for the elemental analysis of the Schiff base complex of copper coated on epoxy-modified Fe₃O₄@SiO₂ MNPs.^{52–55}

Catalyst Preparation. The Schiff base complex of copper was successfully coated on epoxy-modified Fe₃O₄@SiO₂ MNPs according to the following steps.

Preparation of Fe₃O₄. To prepare Fe₃O₄, we used the coprecipitation method. First, FeSO₄·7H₂O (0.9 g) and FeCl₃ (0.97 g) with 120 mL of distilled water were mixed under vigorous stirring at 80 °C, then 120 mL aqueous ammonia solution 1.5 M with a dropping funnel was added dropwise to it, and it immediately turned black. Second, the resulting black mixture was stirred under N₂ gas for 30 min. Next, the reaction mixture was kept for 2.5 h at 25 °C, and the black Fe₃O₄ was isolated using an exterior super magnet and washed four times

with distilled water (4 × 50 mL) and once with acetone (1 × 50 mL) and dried in an oven at 40 °C for 24 h.⁵⁶

Preparation of Fe₃O₄@SiO₂. Fe₃O₄ (1 g) in a mixture of ethanol:distilled water (80:20; 100 mL) was dispersed by sonification for 30 min. In sequence, 2 mL of tetraethyl orthosilicate (TEOS) and 2 mL of NH₄OH 25% was added and the resulting solution was kept under N₂ for 12 h. Finally, the resulting products was collected by an external magnetic field and washed five times with distilled water (5 × 50 mL) and once with ethanol (1 × 50 mL). Eventually, the Fe₃O₄@SiO₂ was synthesized and dried in an oven at 40 °C for 24 h.⁵⁷

Preparation of Fe₃O₄@SiO₂@GPTMS. Tural and colleagues have reported the Fe₃O₄@SiO₂@GPTMS from GPTMS functionalized with Fe₃O₄@SiO₂ with a facile strategy.⁴⁵ For this, 1 g of Fe₃O₄@SiO₂ was dispersed in 100 mL of anhydrous toluene for 20 min. In sequence, GPTMS (10 mmol) was added gradually to the Fe₃O₄@SiO₂ solution and was refluxed under nitrogen at 80 °C for 8 h. Finally, the Fe₃O₄@SiO₂@GPTMS was filtered by an external magnet field and washed twice with benzene (2 × 50 mL) and then dried overnight at room temperature.

Preparation of Fe₃O₄@SiO₂@GPTMS/EDA. The Fe₃O₄@SiO₂@GPTMS/EDA compound was prepared easily. A total of 1 g of Fe₃O₄@SiO₂@GPTMS was dispersed in 100 mL of anhydrous toluene for 20 min. Then, ethylenediamine (12 mmol) was added to the Fe₃O₄@SiO₂@GPTMS solution under N₂ at reflux conditions for 24 h. Then, the Fe₃O₄@SiO₂@GPTMS/EDA was filtered by employing an external magnet, washed with benzene (2 × 50 mL), and then dried overnight at room temperature.

Preparation of Fe₃O₄@SiO₂@GPTMS/Schiff Base. First, Fe₃O₄@SiO₂@GPTMS/EDA was dispersed in 50 mL anhydrous toluene for 15 min. Then, the solution of salicylaldehyde (10 mmol) in anhydrous toluene (10 mL) was added dropwise into solution of Fe₃O₄@SiO₂@GPTMS/EDA (1 g) under N₂ at reflux conditions for 24 h. Then, the precipitate (Fe₃O₄@SiO₂@GPTMS/Schiff base) was collected from the solution employing an external magnet, washed with benzene and ethanol several times, and dried overnight at room temperature.

Preparation of the Schiff Base Complex of Copper Coated on Epoxy-Modified Fe₃O₄@SiO₂ MNPs. To synthesize the Schiff base complex of copper coated on epoxy-modified

Fe₃O₄@SiO₂ MNPs, first, Fe₃O₄@SiO₂@GPTMS/Schiff base (1 g) was dispersed in absolute ethanol (30 mL). Afterward, the solution of Cu(NO₃)₂·3H₂O (2.5 mmol) in absolute ethanol (20 mL) was added quickly to the solution of Fe₃O₄@SiO₂@GPTMS/Schiff base under vigorous stirring under reflux conditions for 24 h. Finally, the mixture was gathered employing an exterior magnet, washed several times with water and ethanol, and dried at room temperature to give the Schiff base complex of copper coated on epoxy-modified Fe₃O₄@SiO₂ MNPs.

General Process to Synthesize 2-Amino-4H-Chromene Derivatives Using the Schiff Base Complex of Copper Coated on Epoxy-Modified Fe₃O₄@SiO₂ MNPs. In round-bottom flask, a variety of aldehydes (1 mmol), various phenols (1 mmol), malononitrile (1 mmol), nanocatalyst (0.05 g), and ethanol (5 mL) were reacted under reflux conditions (Table 2). The reaction completion process was investigated using thin layer chromatography. After the completion of the reaction, the reaction mixture was cooled to 25 °C. Subsequently, the magnetic catalyst was recovered from the reaction mixture by an exterior super magnet, washed with ethanol, and dried in an oven for 24 h. The solid product came through simple filtration and washed with ethanol thoroughly for purification and dried at room temperature. Various chromene-annulated heterocycles were specified using FT-IR, melting point, ¹H NMR, and ¹³C NMR techniques.

Compound 4a. Orange solid, FT-IR (KBr, cm⁻¹): 3403, 3325, 3192, 2936, 2199, 1687, 1671, 1450, 1070, 719. ¹H NMR (250 MHz, DMSO-*d*₆) δ: 7.19–8.01 (m, 11H, Ar–H, NH₂), 4.57 (s, 1H, C–H). ¹³C NMR (62.5 MHz, DMSO-*d*₆) δ: 36.9, 57.9, 119.7, 122.4, 126.2, 126.5, 127.5, 128.1, 129, 131, 131.4, 134.5, 134.9, 144, 149.3, 158.8, 177.2, 182.9.

Compound 4b. Orange solid; FT-IR (KBr, cm⁻¹): 3401, 3331, 3196, 3072, 2922, 2204, 1493, 1411, 1301, 1246, 1183, 859, 780 cm⁻¹. ¹H NMR (250 MHz, DMSO-*d*₆) δ: 7.46–8.04 (m, 8H, Ar–H), 8.12–8.15 (s, 2H), 4.77 (s, 1H). ¹³C NMR (62.5 MHz, DMSO-*d*₆) δ: 36.8, 56.7, 119.4, 121, 124.2, 126.2, 126.5, 129.5, 131.1, 131.3, 134.6, 134.9, 146.9, 149.8, 151.4, 158.8, 177.1, 182.9.

Compound 4c. Orange solid, FT-IR (KBr, cm⁻¹): 3408, 3218, 2199, 1662, 1635, 1405, 1243, 1073, 734. ¹H NMR (250 MHz, DMSO-*d*₆) δ: 7.06–8.01 (m, 10H, Ar–H, NH₂), 2.47 (s, 3H, Me), 4.54 (s, 1H, C–H). ¹³C NMR (62.5 MHz, DMSO-*d*₆) δ: 21, 36.5, 58, 119.8, 122.6, 126.2, 126.5, 128, 129, 131, 131.4, 134.5, 134.9, 136.7, 141, 149.2, 158.7, 183.

Compound 4d. Red-brown solid, FT-IR (KBr, cm⁻¹): 3409, 3329, 3191, 2193, 1674, 1637, 1529, 1475, 1366, 948. ¹H NMR (250 MHz, DMSO-*d*₆) δ: 7.46–8.05 (m, 9H, Ar–H, NH₂), 4.79 (s, 1H, C–H). ¹³C NMR (62.5 MHz, DMSO-*d*₆) δ: 36.2, 56.7, 119.3, 120.4, 123.6, 124.9, 126.2, 126.4, 131.1, 131.4, 131.9, 133.6, 134.6, 134.9, 145.3, 148.3, 150.0, 158.7, 177.2, 183.0.

Compound 4e. Red-brown solid, FT-IR (KBr, cm⁻¹): 3467, 3340, 3194, 2922, 2202, 1733, 1670, 1469, 1400, 1365, 1248, 717 cm⁻¹. ¹H NMR (250 MHz, DMSO-*d*₆) δ: 7.29–8.04 (m, 10H, Ar–H, NH₂), 5.10 (s, 1H, C–H). ¹³C NMR (62.5 MHz, DMSO-*d*₆) δ: 33.5, 56.1, 119.1, 121.1, 126.2, 126.5, 128.4, 129.1, 131, 131.3, 132.3, 132.7, 133.3, 134.6, 135, 140.6, 150, 158.8, 177.2, 182.9.

Compound 4f. Dark-orange solid, FT-IR (KBr, cm⁻¹): 3398, 3318, 3006, 2883, 2199, 1686, 1634, 1443, 1245, 923, 772. ¹H NMR (250 MHz, DMSO-*d*₆) δ: 8.0–8.02 (m, 1H, Ar–H), 7.83–7.84 (m, 3H, Ar–H), 7.22 (s, 2H, NH₂), 7.04–

7.07 (d, 2H, ³J = 8.5 Hz, Ar–H), 6.59–6.30 (d, 2H, ³J = 8.5 Hz, Ar–H), 4.46 (s, 1H, C–H), 2.47–2.81 (s, 6H, 2 Me). ¹³C NMR (62.5 MHz, DMSO-*d*₆) δ: 35.8, 58.3, 112.8, 119.9, 123.1, 126.2, 126.4, 128.7, 130.9, 131.5, 134.5, 134.9, 148.6, 149.9, 158.7, 177.4, 183.0.

Compound 4g. Orange solid, FT-IR (KBr, cm⁻¹): 3413, 3329, 3118, 2921, 2862, 2197, 1689, 1416, 1210, 742. ¹H NMR (250 MHz, DMSO-*d*₆) δ: 7.82–8.01 (m, 5H, Ar–H), 7.40–7.50 (m, 3H, Ar–H), 6.26–6.33 (s, 2H, NH₂), 4.73 (s, 1H, C–H). ¹³C NMR (62.5 MHz, DMSO-*d*₆) δ: 30.3, 54.9, 106.8, 111.1, 119.6, 120.2, 126.3, 126.6, 130.9, 131.3, 134.6, 135.1, 142.8, 149.6, 154.9, 159.6, 177.2, 182.6.

Compound 4h. Brown solid, FT-IR (KBr, cm⁻¹): 3438, 3334, 3191, 3059, 2232, 2196, 1667, 1597, 1403, 1241, 1073, 716, 615. ¹H NMR (250 MHz, DMSO-*d*₆) δ: 7.98 (m, 1H, Ar–H), 7.50–7.75 (m, 6H, Ar–H), 7.40 (m, 3H, Ar–H and NH₂), 4.67 (s, 1H). ¹³C NMR (62.5 MHz, DMSO-*d*₆) δ: 37.0, 56.9, 110.3, 119.1, 119.4, 121.1, 126.2, 126.4, 129.2, 131.0, 131.3, 132.9, 134.6, 134.9, 149.3, 149.8, 158.8, 177.1, 182.9.

Compound 4j. Brick red solid, FT-IR (KBr, cm⁻¹): 3444, 3060, 2931, 2194, 1671, 1457, 1246, 724. ¹H NMR (250 MHz, DMSO-*d*₆) δ: 8.50 (d, 1H, Ar–H), 7.21–8.06 (m, 13H, Ar–H, NH₂), 5.58 (s, 1H, C–H). ¹³C NMR (62.5 MHz, DMSO-*d*₆) δ: 31.2, 58.5, 119.7, 123.3, 124.0, 126.3, 126.7, 127.8, 128.8, 131.0, 131.3, 133.7, 134.6, 134.9, 141.6, 149.8, 158.7, 177.3, 183.0.

Compound 4k. Orange solid, FT-IR (KBr, cm⁻¹): 3378, 2976, 2215, 1707, 1663, 1475, 1214, 762. ¹H NMR (250 MHz, DMSO-*d*₆) δ: 7.35–8.05 (m, 14H, Ar–H, NH₂), 4.77 (s, 1H, C–H). ¹³C NMR (62.5 MHz, DMSO-*d*₆) δ: 37.2, 57.8, 119.8, 122.1, 126.5, 127.9, 128.1, 128.7, 131.0, 131.4, 132.6, 133.3, 134.5, 134.9, 141.5, 149.4, 158.7, 177.3, 183.0.

Compound 4l. Brown solid, FT-IR (KBr, cm⁻¹): 3413, 3349, 3062, 2197, 1688, 1673, 1457, 1247, 960, 726. ¹H NMR (250 MHz, DMSO-*d*₆) δ: 8.57 (s, 1H, Ar–H), 7.62–8.52 (m, 7H, Ar–H), 7.41 (s, 2H, NH₂), 4.68 (s, 1H, C–H). ¹³C NMR (62.5 MHz, DMSO-*d*₆) δ: 34.7, 57.0, 119.5, 121.1, 124.3, 126.2, 126.4, 131.1, 131.3, 134.6, 134.9, 136.2, 139.7, 148.3, 148.8, 149.1, 149.7, 158.8, 177.1, 183.0.

Compound 6a. White solid, FT-IR (KBr, cm⁻¹): 3432, 3339, 2182, 1651, 1452, 1245, 1027, 753. ¹H NMR (250 MHz, DMSO-*d*₆) δ: 7.86 (m, 3H, Ar–H), 7.16–7.36 (m, 8H, Ar–H), 6.94 (s, 2H, NH₂), 5.24 (s, 1H, C–H). ¹³C NMR (62.5 MHz, DMSO-*d*₆) δ: 38.4, 58.31, 116.1, 117.2, 120.9, 124.0, 125.3, 127.0, 127.4, 128.8, 129.1, 129.9, 130.5, 131.2, 146.1, 147.2, 160.1.

Compound 6c. White solid, FT-IR (KBr, cm⁻¹): 3445, 3304, 3166, 2872, 2226, 2184, 1652, 1586, 1468, 1405, 1238, 1083, 807, 780, 620, 558. ¹H NMR (250 MHz, DMSO-*d*₆) δ: 5.41 (s, 1H), 7.12 (s, 2H, NH₂), 7.34 (m, 5H, Ar–H), 7.63–7.71 (m, 3H, Ar–H), 7.85 (m, 2H, Ar–H). ¹³C NMR (62.5 MHz, DMSO-*d*₆) δ: 38.3, 57.2, 109.9, 114.8, 117.2, 119.0, 123.7, 125.4, 127.7, 128.4, 128.9, 130.3, 131.2, 133.1, 147.3, 151.3, 160.3.

Compound 8a. Brown solid, FT-IR (KBr, cm⁻¹): 3505, 3429, 2192, 1651, 1619, 1450, 1148; ¹H NMR (250 MHz, DMSO-*d*₆) δ: 9.68 (s, 1H, OH), 7.14–7.25 (m, 5H, Ar–H), 6.75–6.83 (m, 3H, Ar–H), 6.38–6.45 (s, 2H, NH₂), 3.35 (s, 1H, C–H). ¹³C NMR (62.5 MHz, DMSO-*d*₆) δ: 56.6, 102.6, 112.8, 114.1, 121.1, 127.0, 127.8, 129.0, 130.4, 146.8, 149.2, 157.5, 160.6.

Compound 8b. Dark brown solid, FT-IR (KBr, cm⁻¹): 3442, 3328, 3195, 3079, 2979, 2193, 1644, 1579, 1471, 1350,

1155, 857, 734. ^1H NMR (250 MHz, DMSO- d_6) δ : 9.77 (s, 1H, OH), 8.03 (t, 1H, J = 7.8 Hz, Ar-H), 6.99 (s, 2H, NH₂), 4.87 (s, 1H, CH), 7.59 (d, 2H, J = 9.25, Ar-H), 6.81 (d, 2H, J = 8 Hz, Ar-H), 6.44–6.49 (m, 2H, Ar-H). ^{13}C NMR (62.5 MHz, DMSO- d_6) δ : 18.9, 55.8, 56.5, 102.8, 112.9, 113.1, 120.7, 122.2, 130.3, 130.7, 134.7, 148.3, 148.9, 149.3, 157.9, 160.9.

■ ASSOCIATED CONTENT

SI Supporting Information

The Supporting Information is available free of charge at <https://pubs.acs.org/doi/10.1021/acsomega.1c03672>.

Copies of FT-IR, ^1H NMR (250 MHz, DMSO- d_6), and ^{13}C NMR (62.5 MHz, DMSO- d_6) spectra of synthesized compounds (PDF)

■ AUTHOR INFORMATION

Corresponding Author

Ali Ramazani – Department of Chemistry, Faculty of Science, University of Zanjan, Zanjan 45371-38791, Iran; Department of Biotechnology, Research Institute of Modern Biological Techniques (RIMBT), University of Zanjan, Zanjan 45371-38791, Iran; orcid.org/0000-0003-3072-7924; Email: aliramazani@znu.ac.ir, aliramazani@gmail.com

Authors

Sobhan Rezayati – Department of Chemistry, Faculty of Science, University of Zanjan, Zanjan 45371-38791, Iran
Sami Sajjadifar – Department of Chemistry, Payame Noor University, 19395-4697 Tehran, Iran
Hamideh Aghahosseini – Department of Chemistry, Faculty of Science, University of Zanjan, Zanjan 45371-38791, Iran
Aram Rezaei – Nano Drug Delivery Research Center, Health Technology Institute, Kermanshah University of Medical Sciences, Kermanshah 1673-67145, Iran; orcid.org/0000-0003-2408-7254

Complete contact information is available at: <https://pubs.acs.org/doi/10.1021/acsomega.1c03672>

Notes

The authors declare no competing financial interest.

■ ACKNOWLEDGMENTS

The present study, derived from the Ph.D. thesis by Sobhan Rezayati, was supported by the Iran National Science Foundation INSF and University of Zanjan.

■ REFERENCES

- (1) (a) Yadav, L. D. S.; Singh, S.; Rai, V. K. Catalyst-free, step and pot economic, efficient mercaptoacetylation cyclisation in H₂O: synthesis of 3-mercaptocoumarins. *Green Chem.* **2009**, *11*, 878–882. (b) Rezayati, S.; Salehi, E.; Hajinasiri, R.; Abad, S. A. S. Acetic acid functionalized ionic liquid systems: An efficient and recyclable catalyst for the regioselective ring opening of epoxides with NaN₃. *C. R. Chim.* **2017**, *20*, 554–558. (c) Rezayati, S.; Hajinasiri, R.; Erfani, Z. Microwave-assisted green synthesis of 1,1-diacetates (acylals) using selectfluorTM as an environmental-friendly catalyst under solvent-free conditions. *Res. Chem. Intermed.* **2016**, *42*, 2567–2576. (d) Hajinasiri, R.; Rezayati, S. Solvent-free Synthesis of 1,2-Disubstituted Derivatives of 1,2-Dihydroisoquinoline, 1,2-Dihydroquinoline and 1,2-Dihydropyridine. *Z. Naturforsch., B* **2013**, *68*, 818–822.
- (2) Meyer, A.; Hansen, D. B.; Gomes, C. S. G.; Hobbey, T. J.; Thomas, O. R. T.; Franzreb, M. Preparation and characterization of surface modified γ -Fe₂O₃ (maghemite)-silica nanocomposites used for the purification of benzaldehyde lyase. *Biotechnol. Prog.* **2005**, *21*, 244–254.
- (3) Lu, A.-H.; Schmidt, W.; Matoussevitch, N.; Bönemann, H.; Spliethoff, B.; Tesche, B.; Bill, E.; Kiefer, W.; Schüth, F. Nano-engineering of a Magnetically Separable Hydrogenation Catalyst. *Angew. Chem.* **2004**, *116*, 4403–4406.
- (4) Weissleder, R.; Bogdanov, A.; Neuwelt, E. A.; Papisov, M. Long-circulating iron oxides for MR imaging. *Adv. Drug Delivery Rev.* **1995**, *16*, 321–334.
- (5) Hiergeist, R.; Andrä, W.; Buske, N.; Hergt, R.; Hilger, I.; Richter, U.; Kaiser, W. Application of magnetite ferrofluids for hyperthermia. *J. Magn. Magn. Mater.* **1999**, *201*, 420–422.
- (6) Jordan, A.; Scholz, R.; Wust, P.; Fähling, H.; Felix, R. Magnetic fluid hyperthermia (MFH): Cancer treatment with AC magnetic field induced excitation of biocompatible superparamagnetic nanoparticles. *J. Magn. Magn. Mater.* **1999**, *201*, 413–419.
- (7) Pankhurst, Q. A.; Connolly, J.; Jones, S. K.; Dobson, J. Applications of magnetic nanoparticles in biomedicine. *J. Phys. D: Appl. Phys.* **2003**, *36*, R167–R181.
- (8) del Campo, A.; Sen, T.; Lellouche, J.-P.; Bruce, I. J. Multifunctional magnetite and silica-magnetite nanoparticles: Synthesis, surface activation and applications in life sciences. *J. Magn. Magn. Mater.* **2005**, *293*, 33–40.
- (9) Wang, D.; He, J.; Rosenzweig, N.; Rosenzweig, Z. Superparamagnetic Fe₂O₃ Beads–CdSe/ZnS Quantum Dots Core–Shell Nanocomposite Particles for Cell Separation. *Nano Lett.* **2004**, *4*, 409–413.
- (10) Hyeon, T. Chemical synthesis of magnetic nanoparticles. *Chem. Commun.* **2003**, 927–934.
- (11) Perez, J. M.; Simeone, F. J.; Saeki, Y.; Josephson, L.; Weissleder, R. Viral-Induced Self-Assembly of Magnetic Nanoparticles Allows the Detection of Viral Particles in Biological Media. *J. Am. Chem. Soc.* **2003**, *125*, 10192–10193.
- (12) (a) Abbasi, Z.; Rezayati, S.; Bagheri, M.; Hajinasiri, R. Preparation of a novel, efficient, and recyclable magnetic catalyst, γ -Fe₂O₃@HAP-Ag nanoparticles, and a solvent- and halogen-free protocol for the synthesis of coumarin derivatives. *Chin. Chem. Lett.* **2017**, *28*, 75–82. (b) Sajjadifar, S.; Rezayati, S.; Arzhegar, Z.; Abbaspour, S.; Torabi Jafroudi, M. Applications of iron and nickel immobilized on hydroxyapatite-core-shell γ -Fe₂O₃ as a nanomagnetic catalyst for the chemoselective oxidation of sulfides to sulfoxides under solvent-free conditions. *J. Chin. Chem. Soc.* **2018**, *65*, 960–969. (c) Rezayati, S.; Jafroudi, M. T.; Rezaee Nezhad, E.; Hajinasiri, R.; Abbaspour, S. Imidazole-functionalized magnetic Fe₃O₄ nanoparticles: an efficient, green, recyclable catalyst for one-pot Friedländer quinoline synthesis. *Res. Chem. Intermed.* **2016**, *42*, 5887–5898. (d) Sajjadifar, S.; Rezayati, S.; Shahriari, A.; Abbaspour, S. Silver, iron, and nickel immobilized on hydroxyapatite-core-shell γ -Fe₂O₃ MNPs catalyzed one-pot five-component reactions for the synthesis of tetrahydropyridines by tandem condensation of amines, aldehydes, and methyl acetoacetate. *Appl. Organomet. Chem.* **2018**, *32*, No. e4172. (e) Ezzatzadeh, E. Chemoselective oxidation of sulfides to sulfoxides using a novel Zn-DABCO functionalized Fe₃O₄ MNPs as highly effective nanomagnetic catalyst. *Asian J. Nanosci. Mater.* **2021**, *4*, 125–136. (f) Yadollahzadeh, K. Synthesis of 5-arylmethylene-pyrimidine-2,4,6-trione and 2-arylidene-malononitriles derivatives using a new Brønsted acid nano magnetic catalyst. *Asian J. Nanosci. Mater.* **2021**, *4*, 81–94.
- (13) Ribeiro, R. S.; Silva, A. M. T.; Figueiredo, J. L.; Faria, J. L.; Gomes, H. T. Catalytic wetperoxide oxidation: a route towards the application of hybrid magnetic carbon nanocomposites for the degradation of organic pollutants, A review. *Appl. Catal., B* **2016**, *187*, 428–460.
- (14) Verma, M. L.; Puri, M.; Barrow, C. J. Recent trends in nanomaterials immobilised enzymes for biofuel production. *Crit. Rev. Biotechnol.* **2016**, *36*, 108–119.

- (15) Majouga, A.; Sokolsky-Papkov, M.; Kuznetsov, A.; Lebedev, D.; Efremova, M.; Beloglazkina, E.; Rudakovskaya, P.; Veselov, M.; Zyk, N.; Golovin, Y.; Klyachko, N.; Kabanov, A. Enzyme-functionalized gold-coated magnetite nanoparticles as novel hybrid nanomaterials: synthesis, purification and control of enzyme function by low-frequency magnetic field. *Colloids Surf., B* **2015**, *125*, 104–109.
- (16) Sheoran, A.; Kaur, L.; Kaur, P.; Kumar, V.; Tikoo, K. B.; Agarwal, J.; Bansal, S.; Singhal, S. Graphene based magnetic nanohybrids as promising catalysts for the green synthesis of β -amino alcohol derivatives. *J. Mol. Struct.* **2020**, *1204*, 127522.
- (17) Raj, T.; Bhatia, R. K.; Kapur, A.; Sharma, M.; Saxena, A. K.; Ishar, M. P. S. Cytotoxic activity of 3-(5-phenyl-3H-[1,2,4]dithiazol-3-yl)chromen-4-ones and 4-oxo-4H-chromene-3-carbothioic acid N-phenylamides. *Eur. J. Med. Chem.* **2010**, *45*, 790–794.
- (18) Mohr, S. J.; Chirigos, M. A.; Fuhrman, F. S.; Pryor, J. W. Pyran Copolymer as an Effective Adjuvant to Chemotherapy against a Murine Leukemia and Solid Tumor. *Cancer Res.* **1975**, *35*, 3750–3754.
- (19) Moon, D.-Q.; Kim, K.-C.; Jin, C.-Y.; Han, M.-H.; Park, C.; Lee, K.-J.; Park, Y.-M.; Choi, Y. H.; Kim, G.-Y. Inhibitory effects of eicosapentaenoic acid on lipopolysaccharide-induced activation in BV2 microglia. *Int. Immunopharmacol.* **2007**, *7*, 222–229.
- (20) Kaur, R.; Naaz, F.; Sharma, S.; Mehndiratta, S.; Gupta, M. K.; Bedi, P. M. S.; Nepali, K. Screening of a library of 4-aryl/heteroaryl-4H-fused pyrans for xanthine oxidase inhibition: synthesis, biological evaluation and docking studies. *Med. Chem. Res.* **2015**, *24*, 3334–3349.
- (21) Rueping, M.; Sugiono, E.; Merino, E. Asymmetric organocatalysis: an efficient enantioselective access to benzopyranes and chromenes. *Chem. – Eur. J.* **2008**, *14*, 6329–6332.
- (22) Bonsignore, L.; Loy, G.; Secci, D.; Calignano, A. Synthesis and pharmacological activity of 2-oxo-(2H) 1-benzopyran-3-carboxamide derivatives. *Eur. J. Med. Chem.* **2013**, *28*, 517–520.
- (23) Martínez-Grau, A.; Marco, J. Friedländer reaction on 2-amino-3-cyano-4H-pyrans: Synthesis of derivatives of 4H-pyran [2,3-b]quinoline, new tacrine analogues. *Bioorg. Med. Chem. Lett.* **1997**, *7*, 3165–3170.
- (24) Amr, A. G. E.; Mohamed, A. M.; Mohamed, S. F.; Abdel-Hafez, N. A.; Hammam, A. E. F. G. Anticancer activities of some newly synthesized pyridine, pyrane, and pyrimidine derivatives. *Bioorg. Med. Chem.* **2006**, *14*, 5481–5488.
- (25) Smith, C. W.; Bailey, J. M.; Billingham, M. E. J.; Chandrasekhar, S.; Dell, C. P.; Harvey, A. K.; Hicks, C. A.; Kingston, A. E.; Wishart, G. N. The anti-rheumatic potential of a series of 2,4-di-substituted-4H-naphtho[1,2-b]pyran-3-carbonitriles. *Bioorg. Med. Chem.* **1995**, *5*, 2783–2788.
- (26) Andreani, L. L.; Lapi, E. On some new esters of coumarin-3-carboxylic acid with balsamic and bronchodilator action. *Boll. Chim. Farm.* **1960**, *99*, 583–586.
- (27) Schiemann, K.; Finsinger, D.; Zenke, F.; Amendt, C.; Knöchel, T.; Bruge, D.; Buchstaller, H. P.; Emde, U.; Stähle, W.; Anzali, S. The discovery and optimization of hexahydro-2H-pyrano[3,2-c]quinolines (HHPQs) as potent and selective inhibitors of the mitotic kinesin-5. *Bioorg. Med. Chem. Lett.* **2010**, *20*, 1491–1495.
- (28) Matteelli, A.; Carvalho, A. C. C.; Dooley, K. E.; Kritski, A. TMC207: the first compound of a new class of potent anti-tuberculosis drugs. *Future Microbiol.* **2010**, *5*, 849–858.
- (29) Kishore, N.; Mishra, B. B.; Tripathi, V.; Tiwari, V. K. Alkaloids as potential anti-tubercular agents. *Fitoterapia* **2009**, *80*, 149–163.
- (30) Mehellou, Y.; De Clercq, E. Twenty-Six Years of Anti-HIV Drug Discovery: Where Do We Stand and Where Do We Go? *J. Med. Chem.* **2009**, *53*, 521–538.
- (31) Ballini, R.; Bosica, G.; Conforti, M. L.; Maggi, R.; Mazzacani, A.; Righi, P.; Sartori, G. Three-component process for the synthesis of 2-amino-2-chromenes in aqueous media. *Tetrahedron* **2001**, *57*, 1395–1398.
- (32) Han, Y. F.; Xia, M. Multicomponent Synthesis of Cyclic Frameworks on Knoevenagel-Initiated Domino Reactions. *Curr. Org. Chem.* **2010**, *14*, 379–413.
- (33) Peng, Y.; Song, G. Amino-functionalized ionic liquid as catalytically active solvent for microwave-assisted synthesis of 4H-pyrans. *Catal. Commun.* **2007**, *8*, 111–114.
- (34) Abdolmohammadi, S.; Balalaie, S. Novel and efficient catalysts for the one-pot synthesis of 3,4-dihydropyrano[c]chromene derivatives in aqueous media. *Tetrahedron Lett.* **2007**, *48*, 3299–3303.
- (35) Nagabhushana, H.; Saundalkar, S. S.; Muralidhar, L.; Nagabhushana, B. M.; Giriya, C. R.; Nagaraja, D.; Pasha, M. A.; Jayashankara, V. P. α -Fe₂O₃ nanoparticles: An efficient, inexpensive catalyst for the one-pot preparation of 3,4-dihydropyrano[c]-chromenes. *Chin. Chem. Lett.* **2011**, *22*, 143–146.
- (36) Heravi, M. M.; Jani, B. A.; Derikvand, F.; Bamoharram, F. F.; Oskooie, H. A. Three component, one-pot synthesis of dihydropyrano[3,2-c]chromene derivatives in the presence of H₆P₂W₁₈O₆₂·18H₂O as a green and recyclable catalyst. *Catal. Commun.* **2008**, *10*, 272–275.
- (37) Jin, T. S.; Liu, L. B.; Zhao, Y.; Li, T. S. Clean, One-Pot Synthesis of 4H-Pyran Derivatives Catalyzed by Hexadecyltrimethyl Ammonium Bromide in Aqueous Media. *Synth. Commun.* **2005**, *35*, 1859–1863.
- (38) Babu, N. S.; Pasha, N.; Rao, K. T. V.; Sai, P. S. S.; Lingaiah, N. A heterogeneous strong basic Mg/La mixed oxide catalyst for efficient synthesis of polyfunctionalized pyrans. *Tetrahedron Lett.* **2008**, *49*, 2730–2733.
- (39) Niknam, K.; Piran, A. Silica-Grafted Ionic Liquids as Recyclable Catalysts for the Synthesis of 3,4-Dihydropyrano[c]chromenes and Pyrano[2,3-c]pyrazoles. *Green Sustain. Chem.* **2013**, *03*, 1–8.
- (40) Kumar, B. S.; Srinivasulu, N.; Udupi, R. H.; Rajitha, B.; Reddy, Y. T.; Reddy, P. N.; Kumar, P. S. An efficient approach towards three component coupling of one pot reaction for synthesis of functionalized benzopyrans. *J. Heterocyclic Chem.* **2006**, *43*, 1691–1693.
- (41) Pourkazemi, A.; Nasouri, Z.; Fakhraie, F.; Razzaghi, A.; Parhami, A.; Zare, A. Efficient production of 2-amino-4H-chromenes and 14-aryl-14H-dibenzo[a, j]xanthenes catalyzed by N, N-diethyl-N-sulfoethanaminium hydrogen sulfate. *Asian J. Nanosci. Mater.* **2020**, *3*, 131–137.
- (42) Jin, T.-S.; Xiao, J.-C.; Wang, S.-J.; Li, T.-S.; Song, X.-R. An Efficient and Convenient Approach to the Synthesis of Benzopyrans by a Three-Component Coupling of One-Pot Reaction. *Synlett* **2003**, *2003*, 2001–2004.
- (43) Heravi, M. M.; Bakhtiari, K.; Zadsirjan, V.; Bamoharram, F. F.; Heravi, O. M. Aqua mediated synthesis of substituted 2-amino-4H-chromenes catalyzed by green and reusable Preysslser heteropolyacid. *Bioorg. Med. Chem. Lett.* **2007**, *17*, 4262–4265.
- (44) Chen, L.; Li, Y. Q.; Huang, X. J.; Zheng, W. J. N,N-dimethylamino-functionalized basic ionic liquid catalyzed one-pot multicomponent reaction for the synthesis of 4H-benzo[b]pyran derivatives under solvent-free condition. *Heteroat. Chem.* **2009**, *20*, 91–94.
- (45) Tural, B.; Tural, S.; Ertas, E.; Yalınkılıç, I.; Demir, A. S. Purification and covalent immobilization of benzaldehyde lyase with heterofunctional chelate-epoxy modified magnetic nanoparticles and its carbonylation reactivity. *J. Mol. Catal. B: Enzym.* **2013**, *95*, 41–47.
- (46) Ulu, A.; Ozcan, I.; Koytepe, S.; Ates, B. Design of epoxy-functionalized Fe₃O₄@MCM-41 core-shell nanoparticles for enzyme immobilization. *Int. J. Biol. Macromol.* **2018**, *115*, 1122–1130.
- (47) Xie, H.; Liu, H.; Wang, M.; Pan, H.; Gao, C. L-Tyrosine-Pd complex supported on Fe₃O₄ magnetic nanoparticles: A new catalyst for C–C coupling and Synthesis of sulfides. *Appl. Organomet. Chem.* **2020**, *34*, No. e5256.
- (48) Ghorbani-Choghamarani, A.; Darvishnejad, Z.; Norouzi, M. Cu(II)–Schiff base complex-functionalized magnetic Fe₃O₄ nanoparticles: a heterogeneous catalyst for various oxidation reactions. *Appl. Organomet. Chem.* **2015**, *29*, 170–175.
- (49) Inaloo, I. D.; Majnooni, S.; Eslahi, H.; Esmaeilpour, M. Nickel(II) Nanoparticles Immobilized on EDTA-Modified Fe₃O₄@SiO₂ Nanospheres as Efficient and Recyclable Catalysts for Ligand-Free Suzuki–Miyaura Coupling of Aryl Carbamates and Sulfamates. *ACS Omega* **2020**, *5*, 7406–7417.

(50) Mirzaee, M.; Bahramian, B.; Gholampour, P.; Teymouri, S.; Khorsand, T. Preparation and characterization of Fe_3O_4 @Boehmite core-shell nanoparticles to support molybdenum or vanadium complexes for catalytic epoxidation of alkenes. *Appl. Organomet. Chem.* **2019**, *33*, No. e4792.

(51) Chary, K. V. R.; Srikanth, C. S. Selective Hydrogenation of Nitrobenzene to Aniline over Ru/SBA-15 Catalysts. *Catal. Lett.* **2009**, *128*, 164–170.

(52) Ebrahimiasl, H.; Azarifar, D. Copper-based Schiff Base Complex Immobilized on Coreshell Fe_3O_4 @ SiO_2 as a magnetically recyclable and highly efficient nanocatalyst for green synthesis of 2-amino-4H-chromene derivatives. *Appl. Organomet. Chem.* **2019**, *34*, No. e5359.

(53) Ebrahimiasl, H.; Azarifar, D.; Rakhtshah, J.; Keypour, H.; Mahmoudabadi, M. Application of novel and reusable Fe_3O_4 @CoII(macrocylic Schiff base ligand) for multicomponent reactions of highly substituted thiopyridine and 4H-chromene derivatives. *Appl. Organomet. Chem.* **2020**, *34*, No. e5769.

(54) Khan, M. N.; Pal, S.; Karamthulla, S.; Choudhury, L. H. Imidazole as organocatalyst for multicomponent reactions: diversity oriented synthesis of functionalized hetero- and carbocycles using in situ-generated benzylidenemalononitrile derivatives. *RSC Adv.* **2014**, *4*, 3732–3741.

(55) Hosseinzadeh-Baghan, S.; Mirzaei, M.; Eshtiagh-Hosseini, H.; Zadsirjan, V.; Heravi, M. M.; Mague, J. T. An inorganic–organic hybrid material based on a Keggin type polyoxometalate@Dysprosium as an effective and green catalyst in the synthesis of 2-amino-4H-chromenes via multicomponent reactions. *Appl. Organomet. Chem.* **2020**, *34*, No. e5793.

(56) Yuan, D.; Zhang, Q.; Dou, J. Supported nanosized palladium on superparamagnetic composite microspheres as an efficient catalyst for Heck reaction. *Catal. Commun.* **2010**, *11*, 606–610.

(57) Tajbakhsh, M.; Farhang, M.; Hosseinzadeh, R.; Sarrafi, Y. Nano Fe_3O_4 supported biimidazole Cu(i) complex as a retrievable catalyst for the synthesis of imidazo[1,2-a]pyridines in aqueous medium. *RSC Adv.* **2014**, *4*, 23116–23124.

■ NOTE ADDED AFTER ASAP PUBLICATION

Published ASAP on September 14, 2021; Scheme 1, Scheme 4, and abstract graphic revised September 22, 2021.